Superallowed Gamow-Teller Decay of the Doubly Magic Nucleus ^{100}Sn

C. B. Hinke[1], M. Böhmer[1], P. Boutachkov[2], T. Faestermann[1], H. Geissel[2], J. Gerl[2], R. Gernhäuser[1], M. Górska[2], A. Gottardo[3], H. Grawe[2], J. L. Grębosz[4], R. Krücken[5], N. Kurz[2], Z. Liu[6], L. Maier[1], F. Nowacki[7], S. Pietri[2], Zs. Podolyák[8], K. Sieja[7], K. Steiger[1], K. Straub[1], H. Weick[2], H.-J. Wollersheim[2], P. J. Woods[6], N. Al-Dahan[8], N. Alkhomashi[8], A. Ataç[9], A. Blazhev[10], N. F. Braun[10], I. T. Čeliković[11], T. Davinson[6], I. Dillmann[2], C. Domingo-Pardo[12], P. C. Doornenbal[13], G. de France[14], G. F. Farrelly[8], F. Farinon[2], N. Goel[2], T. C. Habermann[2], R. Hoischen[2], R. Janik[15], M. Karny[16], A. Kaşkaş[9], I. M. Kojouharov[2], Th. Kröll[17], Y. Litvinov[2], S. Myalski[4], F. Nebel[1], S. Nishimura[13], C. Nociforo[2], J. Nyberg[18], A. R. Parikh[19], A. Procházka[2], P. H. Regan[8], C. Rigollet[20], H. Schaffner[2], C. Scheidenberger[2], S. Schwertel[1], P.-A. Söderström[13], S. J. Steer[8], A. Stolz[21], and P. Strmeň[15]

[1]Physik Department E12, Technische Universität München, D-85748 Garching, Germany
[2]GSI Helmholtzzentrum für Schwerionenforschung GmbH, D-64291 Darmstadt, Germany
[3]INFN-LNL Istituto Nazionale di Fisica Nucleare, Laboratori Nazionali di Legnaro, 35020 Legnaro, Italy
[4]The Henryk Niewodniczanski Institute of Nuclear Physics (IFJ PAN), 31-342 Krakow, Poland
[5]TRIUMF Accelerating Science for Canada, Vancouver, BC, V6T 2A3, Canada and Physik Department E12, Technische Universität München, D-85748 Garching, Germany
[6]School of Physics and Astronomy, The University of Edinburgh, Edinburgh, EH9 3JZ, UK
[7]Université de Strasbourg, IPHC, 67037 Strasbourg Cedex, France
[8]Department of Physics, University of Surrey, Guildford, GU2 7XH, UK
[9]Physics Department, Faculty of Science, Ankara University, 06100 Tandogan, Ankara, Turkey
[10]Institute of Nuclear Physics, University of Cologne, D-50937 Köln, Germany
[11]Institute Vinca, University of Belgrade, 11000 Belgrade, Serbia
[12]IFIC, CSIC-University of Valencia, E-46071 Valencia, Spain
[13]RIKEN Nishina Center, Wako, Saitama 351-0198, Japan
[14]Grand Accélérateur National d'Ions Lourds (GANIL), CEA/DSM-CNRS/IN2P3, 14076 Caen, France
[15]Comenius University, 818 06 Bratislava 16, Slovakia
[16]Institute of Experimental Physics, University of Warsaw, PL-00681 Warsaw, Poland
[17]Institut für Kernphysik, Technische Universität Darmstadt, D-64289 Darmstadt, Germany
[18]Department of Physics and Astronomy, Uppsala University, SE-75120 Uppsala, Sweden
[19]Dept. Fisica i Enginyeria Nuclear, Universitat Politecnica de Catalunya (EUETIB), E-08036 Barcelona, Spain
[20]KVI, University of Groningen, 9747AA Groningen, The Netherlands
[21]National Superconducting Cyclotron Laboratory, Michigan State University, East Lansing, MI 48824-1321, USA

Superallowed Gamow-Teller Decay of the Doubly Magic Nucleus ^{100}Sn

C. B. Hinke,[1] M. Böhmer,[1] P. Boutachkov,[2] T. Faestermann,[1] H. Geissel,[2] J. Gerl,[2] R. Gernhäuser,[1] M. Górska,[2] A. Gottardo,[3] H. Grawe,[2] J. L. Gręboszˌ[4] R. Krücken,[5] N. Kurz,[2] Z. Liu,[6] L. Maier,[1] F. Nowacki,[7] S. Pietri,[2] Zs. Podolyák,[8] K. Sieja,[7] K. Steiger,[1] K. Straub,[1] H. Weick,[2] H.-J. Wollersheim,[2] P. J. Woods,[6] N. Al-Dahan,[8] N. Alkhomashi,[8] A. Ataç,[9] A. Blazhev,[10] N. F. Braun,[10] I. T. Čeliković,[11] T. Davinson,[6] I. Dillmann,[1] C. Domingo-Pardo,[12] P. C. Doornenbal,[13] G. de France,[14] G. F. Farrelly,[2] F. Farinon,[2] N. Goel,[2] T. C. Habermann,[2] R. Hoischen,[2] R. Janik,[15] M. Karny,[16] A. Kaşkaş,[9] I. M. Kojouharov,[2] Th. Kröll,[17] Y. Litvinov,[2] S. Myalski,[4] F. Nebel,[1] S. Nishimura,[13] C. Nociforo,[2] J. Nyberg,[18] A. R. Parikh,[19] A. Procházka,[2] P. H. Regan,[8] C. Rigollet,[20] H. Schaffner,[2] C. Scheidenberger,[2] S. Schwertel,[1] P.-A. Söderström,[18] S. J. Steer,[8] A. Stolz,[21] and P. Strmeň[15]

[1]*Physik Department E12, Technische Universität München, D-85748 Garching, Germany*

[2]*gsi*

[3]*lnl*

[4]*kra*

[5]*tri*

[6]*edi*

[7]*str*

[8]*sur*

[9]*ank*

[10]*col*

[11]*bel*

[12]*val*

[13]*rik*

[14]*ganil*

[15]*bra*

[16]*war*

[17]*dar*

[18]*upp*

[19]*bar*

[20]*gro*

[21]*msu*

(Dated: March 31, 2012)

I. SUMMARY

The shell structure of atomic nuclei is associated with magic numbers and originates from the nearly independent motion of neutrons and protons in a mean potential generated by all nucleons. During beta+ decay a proton transforms into a neutron in a previously not fully occupied orbital, emitting a positron-neutrino pair with either parallel or antiparallel spins: Gamow-Teller (GT) or Fermi-transitions, respectively. The strength of GT-transitions depends sensitively on the underlying shell structure. Here we report measurements of half-life and decay-energy for the decay of ^{100}Sn, the heaviest doubly-magic nucleus with equal proton and neutron number. In its beta-decay a large fraction of the strength is observable and we determine the largest GT-strength ever measured in any nuclear beta-decay, establishing the 'superallowed' nature of this GT-transition. The large strength as well as the low energy states in the daughter nucleus ^{100}In are well reproduced by modern large scale shell model calculations.

II. MAIN TEXT

A. Introduction

GT transitions, in which a proton (neutron) is transformed into a neutron (proton) while at the same time possibly flipping its spin, represent an important spin-isospin degree of freedom in atomic nuclei. They play an important role in many astrophysical processes - they govern, for example, electron captures during the core collapse of a supernova. A detailed understanding of GT-transitions will also provide an essential constraint on the neutrino mass, in the event that neutrino-less double-beta decay is ever observed. Most of the GT-strength is found in the collective Gamow-Teller Giant Resonance (GTGR), which is typically a broad structure fragmented over many states. While in charge-exchange reactions on stable nuclei the full GTGR is accessible, the GT-strength in unstable nuclei can, so far, only be studied via β-decay. However, β-decay studies can only observe the fraction of the total GT-strength within the decay energy window. Towards the proton dripline this window becomes larger. Nevertheless, it is still experimentally challenging to detect all small GT-fragments [1, 2]. Thus in most nuclei measuring the full GT-strength is difficult since it is fragmented and only partially accessible in β-decays.

^{100}Sn, the heaviest doubly-magic nucleus with equal proton and neutron number, N=Z=50, provides an experimentally and theoretically very clean and unique situation with respect to GT-transitions. The closed N=50 and Z=50 shells reduce the effect of long-range correlations, decreasing the amount of fragmentation of the GTGR. Theoretical predictions suggest that a single state is dominantly populated in this decay. At the same time the energy window for β-decay is $\sim$ 7.4 MeV [3] and thus most of the GTGR is accessible. Such a situation for a doubly-magic N=Z system is realized nowhere else in the Segrè chart (the Segrè chart arranges the known nuclei in a two-dimensional lattice with neutron number N and proton number Z as x- and y-axes) : ^{16}O and ^{40}Ca are stable nuclei, ^{56}Ni has a too small Q_{EC} value to make the GT-resonance observable in β-decay and beyond ^{100}Sn N=Z nuclei become particle unstable. Also, a recent experiment shows that ^{56}Ni has a much more fragmented GT strength [4] as a result of a less robust N=Z=28 doubly magic shell closure as well as subtle differences in the shell structure (see the methods section for a more detailed discussion). In an extreme single particle picture the only possible GT-transition in ^{100}Sn is the decay of a proton in a completely filled $g_{9/2}$ shell to a neutron in an empty $g_{7/2}$ shell since the $g_{9/2}$ neutron orbital is filled and no levels above Z=50 are occupied. The β-decay of ^{100}Sn is supposed to be enhanced due to the large number of protons occupying the $g_{9/2}$ shell which can decay to the essentially empty neutron $g_{7/2}$ shell. This would lead to a GTGR consisting of only a single 1^+ level with a large GT-strength (B_{GT}) of about 10, taking into account the standard renormalisation factor of 0.75 of the GT matrix element due to configurations outside the model space [5]. This unique situation has been termed "superallowed GT-decay" [6]. Even in more realistic models, including particle-hole correlations, the GT-decay of the ground state of ^{100}Sn is predicted to populate with more than 95% a single 1^+ state in ^{100}In at an excitation energy of about 3 MeV. In these calculations a B_{GT} of around 8-14 [7–10] is obtained, leading to renormalized predictions of 5-7 [8, 10].

The production and study of the decay properties of ^{100}Sn has been the aim of several experiments [12–16], where only a few ^{100}Sn nuclei were uniquely identified. Here we report on a new measurement of the half-life and Q-value from 259 identified ^{100}Sn nuclei resulting in the smallest log-ft value of any β-decay over the nuclear chart and a large GT-strength establishing the robustness of N=Z=50 shell closures. The experimentally observed GT-strength is well described in the state-of-the-art large scale shell model calculations, allowing for an unprecedented large configuration mixing in the case of ^{100}Sn. This ^{100}Sn doubly-

magic shell closure is the benchmark for various topics currently discussed in this mass region, such as spin-aligned pairing in N=Z nuclei, alpha clustering, and the quadrupole collectivity in the Sn isotopic chain.

B. Experimental details

The experiment was performed at the GSI Helmholtzzentrum Darmstadt, Germany. A ^{124}Xe beam of $E_{kin} = 1$ AGeV with one second long spills of $3 \cdot 10^9$ ions every three seconds was directed onto a beryllium target placed in front of the fragment separator (FRS) [17]. Neutron-deficient nuclei were produced via relativistic projectile fragmentation, transmitted to the final FRS focal plane, and identified event-by-event (see Figure 1). The correct identification was verified by observing the γ radiation depopulating known isomers, e.g. the 8^+ isomer in ^{98}Cd. In total 259 ^{100}Sn nuclei were unambiguously identified. This corresponds to a production rate of 0.75 per hour and a cross-section of 5.8 ± 2.1 pb.

The ions were implanted into a stack of highly segmented silicon strip detectors which was surrounded by the RISING array consisting of 105 Germanium detectors arranged in the stopped beam configuration [18] in order to detect γ rays with high efficiency. 163 of the 259 identified ^{100}Sn nuclei were stopped in the 2.1 mm thick implantation layer.

C. Analysis and results

Following a ^{100}Sn implantation in a pixel of the implantation zone of the silicon detector all decay events were recorded that occurred within 15 seconds in this pixel or the directly neighbouring ones. During this correlation time it was possible to assign 126 decay chains to the 163 ^{100}Sn implantations. A maximum likelihood (MLH) analysis with a maximum of three decay events during the correlation time was used to analyze these decay chains. The half-life of ^{100}Sn was deduced as 1.16 ± 0.20 s in the MLH analysis using literature values for the lifetimes of the daughter nuclei. The measurement is much more precise than previous experiments yielding $0.94^{+0.54}_{-0.27}$ s [14] and $0.55^{+0.70}_{-0.31}$ s [16]. In Figure 2 the decay curve for ^{100}Sn is shown.

Figure 3 shows the γ-ray spectrum observed in coincidence with decay events following ^{100}Sn implantations. For the first time discrete γ transitions from the ^{100}Sn decay could be

observed. The five transitions denoted in Figure 3 are associated with the depopulation of excited states in the daughter nucleus ^{100}In.

The statistics were only sufficient to establish a coincidence between the 436 keV and 96 keV transitions and thus it is impossible to deduce an unambiguous level scheme of ^{100}In. Within uncertainties the transitions could have the same intensity, which would allow for a single cascade of five transitions from the excited 1^+ state to the ground state. However, this would lead to an excitation energy of more than 4 MeV, which is higher than the 2.5(5) MeV predicted with realistic shell model calculations (see e.g. [19, 20]). The large uncertainties of the observed intensities also allow for two parallel cascades originating from this 1^+ state.

Figure 4 shows the relevant level scheme for ^{100}In obtained from large scale shell model calculations (LSSM). In this approach ^{100}Sn is not treated as an inert doubly-magic core but excitations across the Z=N=50 shell closures were allowed within the N=4 harmonic oscillator shell (see methods section for details).

The states of two multiplets, that are relevant for the decay, are shown. The states originate from the $\pi g_{9/2}^{-1} \otimes \nu g_{7/2}^{1}$; I^{π}=(1-8)$^+$ and $\pi g_{9/2}^{-1} \otimes \nu d_{5/2}^{1}$; I^{π}=(2-7)$^+$ multiplets. The predictions reflect the observed γ-ray transitions well if the high energy 2048 keV transition populates the lowest 2^+ state, which decays to lower lying states via the 436, 141, and 96 keV transitions ending either in the 6^+ ground state or a low lying isomeric state with unobserved decay. In this scenario the second 2^+ state is populated with the 1297 keV transition and decays to the lower lying 2^+ and 3^+ states. This may lead to a fragmentation of the intensities making it impossible to observe these transitions in the present experiment. This scenario is supported by the measurement of the total γ-ray energy ($E^*_{1^+} = 2.76 \pm 0.43$ MeV) in a former experiment with a BGO-detector [14], the known mass difference of ^{100}Sn and ^{100}In [13], combined with our measured β end-point energy ($E^*_{1^+} = 2.6 \pm 1.0$ MeV) and our observation of a single event of β-delayed proton emission ($E^*_{1^+} = 2.93 \pm 0.34$ MeV). It is fully consistent with the expectation that dominantly a single 1^+ state is populated in the decay. Further details are given in the methods section.

As a key feature of this experiment, the kinetic energy of the decay positrons fully absorbed in the compact silicon detector array was measured. The spectrum resulting from the summed energies deposited by a β-particle in the pixels of the calorimeter up to three seconds after a ^{100}Sn implantation is shown in Figure 5. It was fitted using a MLH analysis based on a single component β-decay phase space function to determine the endpoint energy

in the decay of ^{100}Sn. For the fit of the end point energy only data in the energy region between 400 keV and 2600 keV were used. In the analysis, corrections were applied for the occurrence of converted low energy transitions emitted during the de-excitation of the daughter nucleus ^{100}In, for Bremsstrahlung emitted when the positrons are slowed down, and for the annihilation of positrons in flight before the deposition of their total kinetic energy. The endpoint energy of the β-decay, if populating a single final state in the daughter nucleus ^{100}In, was determined to be 3.29 ± 20 MeV. The corresponding fraction of electron capture decays is 13% of all ^{100}Sn decays.

D. Discussion

Using the measured half-life and the end point energy a log-ft value of $2.62^{+0.13}_{-0.11}$ was extracted, which is the smallest known log-ft value for any β-decay in the nuclear chart. Thus, the Gamow-Teller decay of ^{100}Sn has much larger strength than the known $0^+ \rightarrow 0^+$ superallowed Fermi decays of $N = Z$ nuclei and is indeed a *superallowed Gamow-Teller decay* [21]. This finding is also illustrated in Figure 6 which shows the distribution of log-ft values for allowed Gamow-Teller and Fermi transitions.

The extracted Gamow-Teller strength B_{GT} of the ^{100}Sn ground state decay to the single excited 1^+ state in ^{100}In is $B_{GT} = 9.1^{+2.6}_{-3.0}$. The measured value is extraordinarily large but consistent with the value of $B_{GT} = 5.8^{+5.5}_{-3.2}$ deduced from previous results of Q_{EC} and $T_{1/2}$ [22] within the large error bars of the earlier measurement. The uncertainty of the new B_{GT} value is dominated by the uncertainty of the β endpoint energy. The extraction of the strength was performed under the assumption of the GT-decay into only one final 1^+ state in ^{100}In. However, if other 1^+ states at excitation energies above the observed state would also be populated, the summed GT-strength would only increase while the B_{GT} for the first excited 1^+ state would decrease. It would have been difficult to observe such states since the reduced phase space for higher lying 1^+ states would have lead to a strongly reduced population.

The LSSM calculations, which within the *gds* harmonic oscillator shell take into account most of the long-range correlations across the N=Z=50 doubly magic shell closure and include up to five particle-hole excitations (see methods section for details) yield a total summed GT-strength of all possible final states in the daughter nucleus up to 60 MeV of

$B_{GT} = 8.19$ applying the standard renormalisation due to correlations beyond the $0\hbar\omega$ *gds* space [5].

A GT-strength of $B_{GT} = 7.82$ is predicted in the experimental Q_{EC} window of 7.03(20) MeV. This corresponds to a reduction of the total renormalised GT-strength of the extreme single particle estimate of $B_{GT,ESPM} \approx 10$ by 18% for excitation energies up to 60 MeV and by 22% in the Q_{EC} window. It is due to mixing in the *gds* harmonic oscillator shell, i.e. emptying of the proton $g_{9/2}$ orbital and pre-filling of the neutron $g_{7/2}$ orbital and destructive interference of the four possible combinations of GT-transitions within the g orbit. The occupation numbers of the two orbitals which are linked by the GT-operator directly influence the strength of the transition matrix element.

The calculation predicts that the largest fraction of the strength remains located in the first excited 1^+ state in agreement with earlier calculations [7, 21]. Nevertheless, according to the LSSM calculations performed in this work it is reasonable to consider that several 1^+ states in ^{100}In are populated in the decay of ^{100}Sn. If we take, as an exercise, from the LSSM calculation the four lowest 1^+ states in ^{100}In with their energy splitting and relative GT-strength (see methods section), the value of $B_{GT}(1^+_1) = 9.1^{+2.6}_{-3.0}$ (assuming a single 1^+ state) would be reduced to $B_{GT}(1^+_1) = 7.6^{+2.2}_{-2.5}$ for the first excited 1^+ state using the experimental half-life and β-spectrum. The corresponding summed GT-strength would be $\sum_{i=1}^{4} B_{GT}(1^+_i) = 9.9^{+2.8}_{-3.2}$. Since this exercise only served to gauge the effect of branching on the experimental B_{GT} value, no error for the branching ratios is included.

The LSSM result of $B_{GT} = 5.7$ for the GT-strength of this first excited 1^+ state agrees within the statistical uncertainty with the value $B_{GT} = 7.6^{+2.2}_{-2.5}$ extracted from the experimental log-ft value under the above assumptions. The experimental concentration of most of the GT-strength in the first excited 1^+ state clearly classifies the ^{100}Sn GT-decay as *super-allowed*. This large experimental GT-strength B_{GT} of the transition to the first excited 1^+ state proves that both, the ^{100}Sn ground state and the first excited 1^+ state in ^{100}In, have relatively pure wave functions. As expected, the LSSM calculation reveals wave functions consisting predominantly of the $\pi g^{10}_{9/2} \otimes \nu g^{0}_{7/2}$ (82% probability) and the $\pi g^{9}_{9/2} \otimes \nu g^{1}_{7/2}$ (54% probability) components, respectively. The high purity of the wave functions within the *gds* model space establishes for the first time the simultaneous robustness of the Z=50 and N=50 shell closures in ^{100}Sn only ~ 3 MeV from the proton dripline corroborating for N=50 the results of Refs.[23, 24] and clearly excludes the need for explicitly treating the unbound

proton orbits as continuum states.

The LSSM calculations enable for the first time a large enough configuration mixing in the *gds* shell to obtain converged results which leads to meaningful conclusions in this exotic region far away from the valley of stability. This gives confidence to be able to obtain reliable and more accurate results for nuclei in the neighbourhood of ^{100}Sn, especially close to the proton dripline.

The knowledge of the underlying shell structure of nuclei in the vicinity of ^{100}Sn has to be determined with the highest possible accuracy to answer the burning questions in the nuclear structure, like the possibility of a new coupling scheme which might develop in the N=Z nuclei in the vicinity of ^{100}Sn [25]. The present measurement consists in a stringent test for LSSM calculations, in which the realistic character of such a coupling scheme still needs to be probed.

A better understanding of the nuclear structure is of major importance for modelling weak interaction rates in nuclei, which depend on the underlying shell structure, and play an important role in many astrophysical processes. For example, GT transitions govern electron captures during the core collapse of a supernova explosion of massive stars. The knowledge of GT transitions is also an essential constraint for the theoretical calculations of neutrinoless double-beta decay matrix elements, the knowledge of which is necessary to relate the neutrino mass with the rate of this yet undiscovered process. Further interest in the decay rates of nuclei around ^{100}Sn comes from the study of astrophysical processes, for which this region has been considered as the end of the rapid proton capture process due to the Sn-Sb-Te cycle.

III. METHODS SUMMARY

^{100}Sn and neighbouring nuclei have been produced by fragmentation of a 1.0 A GeV ^{124}Xe beam from the GSI accelerators, separated in the FRS and identified by multiple δE, Bρ and ToF measurements. The nuclei were stopped in an implantation detector with high spatial resolution in order to correlate implantations with succeeding decays. The device was surrounded by the "Stopped Beam Rising" array of 15x7 Ge-detectors in close geometry. In this configuration the setup enabled us to do nearly 4π spectroscopy of the emitted γ and particle decay radiation. With a photo-peak efficiency of about 10% (E=1 MeV) for

γ-ray detection and nearly 100% for full energy detection of decay particles up to 5 MeV, this high resolution setup allowed for a maximum use of the secondary beam.

The extraction of the ^{100}Sn half life and the β endpoint-energy was done in the framework of a maximum likelihood analysis applied to the time distribution of β decays after implantation and the energy distribution of emitted positrons, respectively. This analysis also considered the daughter decays and the presence of uncorrelated random background decays from previous implantations.

For the interpretation of the measured GT-strength and of the observed emitted γ-rays from ^{100}In large scale shell model calculations have been performed. The valence space used in LSSM consists of the N=4 harmonic oscillator shell, i.e. proton and neutron $\pi\nu(g, d, s)$ orbitals outside the ^{80}Zr core. The calculations included up to 5 particle-hole excitations from the $g_{9/2}$ proton and neutron orbitals to the rest of the shell which permitted to obtain converged results for excitation spectra and GT-strength.

---

[1] Ichimura, M., Sakai, H. & Wakasa, T. Spin-isospin responses via (p,n) and (n,p) reactions. *Prog. Part. Nucl. Phys.* **56,** 446-531 (2006).

[2] Hardy, J. C., Carraz, L. C., Jonson, B. & Hansen, P. G. The essential decay of pandemonium: A demonstration of errors in complex beta-decay schemes. *Phys. Lett. B* **71,** 307-310 (1977).

[3] Audi, G., Wapstra, A. H. & Thibault, C. The Ame2003 atomic mass evaluation: (II). Tables, graphs and references. *Nucl. Phys. A* **729,** 337-676 (2003).

[4] Sasano, M. *et al.*, Gamow-Teller transition strengths from ^{56}Ni. *Phys. Rev. Lett.* **107,** 202501 (2011).

[5] Caurier, E., Martínez-Pinedo, G., Nowacki, F., Poves, A. & Zuker, P. A. The shell model as a unified view of nuclear structure. *Rev. Mod. Phys.* **77,** 427-488 (2005).

[6] Brown B. A. The nuclear shell model towards the drip lines. *Prog. Part. Nucl. Phys.* **47,** 517-599 (2001).

[7] Brown B. A. & Rykaczewski, K. Gamow-Teller strength in the region of ^{100}Sn. *Phys. Rev. C* **50,** R2270-R2273 (1994).

[8] Dean, D. J., Koonin, S. E., Kuo, T. T. S., Langanke, K. & Radha, P. B. Complete $0\hbar\omega$ shell model Monte Carlo calculations of ^{94}Ru, ^{96}Pd, ^{96,98}Cd and ^{100}Sn. *Phys. Lett. B* **367,** 17-20

(1996).

[9] Bobyk, A., Kaminski, W. & Borzov, I. N. Gamow-Teller beta-decay strengths of neutron-deficient tin isotopes: Comparison of FFST and pnBCS+QRPA results. *Acta Phys. Pol. B* **31,** 953-963 (2000).

[10] Batist, L. *et al.* Systematics of Gamow-Teller beta decay "Southeast" of ^{100}Sn. *Eur. Phys. J. A* **46,** 45-53 (2010).

[11] Schneider, R. *et al.* Production and identification of ^{100}Sn. *Zeitschr. f. Phys. A* **348,** 241-242 (1994).

[12] Lewitowicz M. *et al.* Identification of the doubly-magic nucleus ^{100}Sn in the reaction ^{112}Sn+^{nat}Ni at 63 MeV/nucleon. *Phys. Lett B* **332,** 20-24 (1994).

[13] Chartier M. *et al.* Mass measurement of ^{100}Sn. *Phys. Rev. Lett.* **77,** 2400-2403 (1996).

[14] Sümmerer K. *et al.* Identification and decay spectroscopy of ^{100}Sn at the GSI projectile fragment separator FRS. *Nucl. Phys. A* **616,** 341c-345c (1997).

[15] Stolz A. *et al.*, Projectile fragmentation of ^{112}Sn at Elab=1A GeV. *Phys. Rev. C* **65,** 064603 (2002).

[16] Bazin D. *et al.*, Production and beta-decay of rp-process nuclei ^{96}Cd, ^{98}In, and ^{100}Sn. *Phys. Rev. Lett.* **101,** 252501 (2008).

[17] Geissel H. *et al.* The GSI projectile fragment separator (FRS): a versatile magnetic system for relativistic heavy ions. *Nucl. Instr. Meth. B* **70,** 286-297 (1992).

[18] Pietri S. *et al.* Recent results in fragmentation isomer spectroscopy with rising. *Nucl. Instrum. Meth. B* **261,** 1079-1083 (2007).

[19] Plettner C. *et al.* Beta decay of ^{100}In. *Phys. Rev. C* **66,** 044319 (2002).

[20] Coraggio, L., Covello, A., Gargano, A. & Itaco, N. Structure of particle-hole nuclei around ^{100}Sn. *Phys. Rev. C* **70,** 034310 (2004).

[21] Hamamoto I. & Sagawa H., Gamow-Teller beta decay and isospin impurity in nuclei near the proton drip line. *Phys. Rev. C* **48,** R960-R963 (1993).

[22] Faestermann T. *et al.* Decay studies of N≈Z nuclei from ^{75}Sr to ^{102}Sn. *Eur. Phys. J. A* **15,** 185-188 (2002).

[23] Blazhev A. *et al.* Observation of a core-excited E4 isomer in ^{98}Cd. *Phys. Rev. C* **69,** 064304 (2004).

[24] Boutachkov P. *et al.* High-spin isomers in ^{96}Ag: Excitations across the Z=38 and Z=50, N=50

closed shells. *Phys. Rev. C* **84,** 044311 (2011).

[25] Cederwall B. *et al.* Evidence for a spin-aligned neutron-proton paired phase from the level structure of ^{92}Pd. *Nature* **469,** 68-71 (2011).

IV. FIGURE LEGENDS

Figure 1:

Title: Particle Identification Plot

Particle identification plot with respect to the nuclear charge Z and the mass-to-charge ratio A/Z for the full statistics of the ^{100}Sn fragment separator setting. In total 259 ^{100}Sn nuclei (indicated) were unambiguously identified. Resolutions (FWHM) in mass of $\Delta A = 0.32$ and nuclear charge $\Delta Z = 0.25$ were obtained.

Figure 2:

Title: Time distribution of first decay events

Observed time distribution of all first decay events after the implantation of ^{100}Sn nuclei occurring in the nearest neighbouring pixels (solid line histogram). Decay curves resulting from the MLH analysis are shown individually for ^{100}Sn (dashed) and its daughter ^{100}In (dash-dotted) together with the sum of these decay curves (solid) taking into account a small amount of random background.

Figure 3:

Title: γ-radiation spectrum

Energy distribution of the γ-radiation observed in coincidence with the β-decay of ^{100}Sn. The range up to 500 keV is shown expanded in the inset. The spectrum contains with a probability of 65% radiation directly following ^{100}Sn decay events. The other contributions are uncorrelated background decays and daughter decays of ^{100}In. None of the observed lines corresponds to known transitions from these minor contributions. The measured absolute intensities of the five lines with the energies 96, 141, 436, 1297 and 2048 keV are 79 ± 40, 100 ± 31, 59 ± 22, 72 ± 26 and 53 ± 26 corrected for conversion assuming M1-transitions and 141 ± 70, 122 ± 37, 59 ± 22, 72 ± 26 and 53 ± 26 assuming E2-transitions.

Figure 4:

Title: Tentative level scheme of ^{100}In

Left: Large scale shell model (LSSM) calculation of the low lying excited states in ^{100}In. Spin, parity and energy in keV is given. Populated levels with almost pure $\pi g_{9/2}^{-1} \otimes \nu g_{7/2}^{1}$ configuration are indicated with bold lines while the remaining levels are part of the $\pi g_{9/2}^{-1} \otimes \nu d_{5/2}^{1}$ multiplet. Relative intensities are shown for selected transitions. *Right:* Most likely level scheme for the observed five γ-transitions in ^{100}In. Since one low energy transition might have been missed the energy of the levels might have a systematic shift of up to $x = 80$ keV. The dashed transitions were not observed.

Figure 5:

Title: Distribution of positron energies

Distribution of the positron energies emitted in the β-decay of ^{100}Sn. The spectrum contains only decay events which can be assigned to ^{100}Sn decays with a probability of at least 75%. The MLH fit was applied to the region between 400 keV and 2600 keV which is indicated with markers. The solid curve illustrates the shape of the best fitting single component β-decay phase space function determined in a MLH analysis.

Figure 6:

Title: Log-ft values from allowed β-decays

Compilation of the log-ft values of allowed nuclear β-decays. The decay of ^{100}Sn is unique since it has the smallest known log-ft value of any β-decay in the nuclear chart.

V. SUPPLEMENTARY INFORMATION

Supplementary Information is linked to the online version of the paper at www.nature.com/nature.

VI. ACKNOWLEDGMENTS

We thank the GSI ion source and accelerator staff for the preparation of a stable high-intensity ^{124}Xe-beam as well as the FRS technicians for setting up the beam line detectors. We would like to acknowledge fruitful discussions with Gabriel Martínez-Pinedo, Karlheinz Langanke and Andres Zuker. We are also grateful to the EUROBALL Owners Committee for the use of the Euroball Cluster Detectors. This work was supported by the BMBF under contracts 06MT238, 06MT9156, 06KY205I and 06KY9136I, by the GSI, by the DFG Cluster of Excellence 153 *Origin and Structure of the Universe*, by the EC within the FP6 through I3-EURONS (contract no. RII3-CT-2004-506065) and by the Swedish Research Council.

VII. AUTHOR CONTRIBUTIONS

Fragment separator: H.W., P.B., H.Ge., M.G., Z.P., C.N.; particle detectors: C.H., K.Str., R.G., T.F., L.M., F.Ne.; RISING γ-array: P.B., M.G., S.P., J.Ge., I.K., H.- J.W.; data acquisition and analysis software: M.B., R.G., J.Gr., N.K., L.M.; data analysis and interpretation: C.H., K.Str., T.F., M.G., H.Gr., R.K., K.Ste., F.No., K.Si.; shell model calculations: F.No., K.Si.; writing of manuscript: C.H., T.F., R.G., H.Gr., R.K., F.No., K.Si.; all authors except H.Gr., F.No., K.Si. took part in the preparation and the beam times and all authors commented on the final paper.

VIII. AUTHOR INFORMATION

Reprints and permissions information is available at www.nature.com/reprints. The authors declare no competing financial interests. Readers are welcome to comment on the online version of this article at www.nature.com/nature. Correspondence and requests for materials should be addressed to T.F. (thomas.faestermann@ph.tum.de).

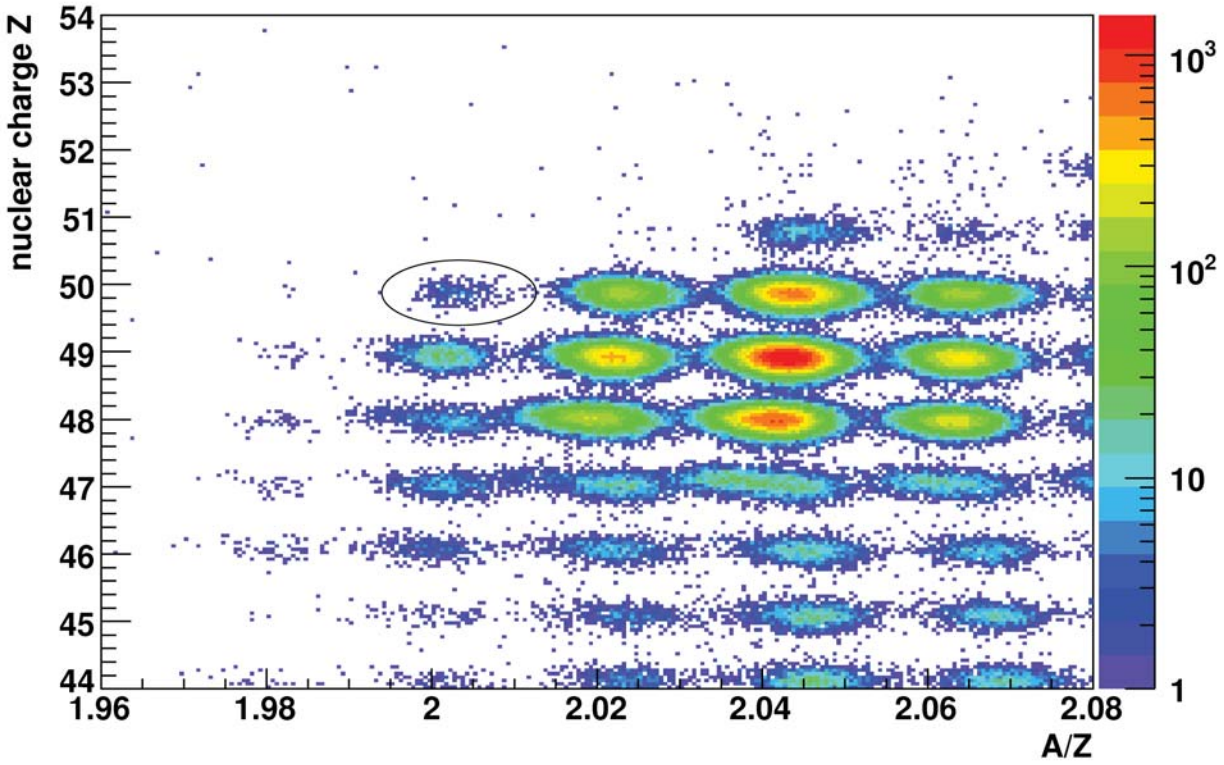

FIG. 1: Title: Particle Identification Plot

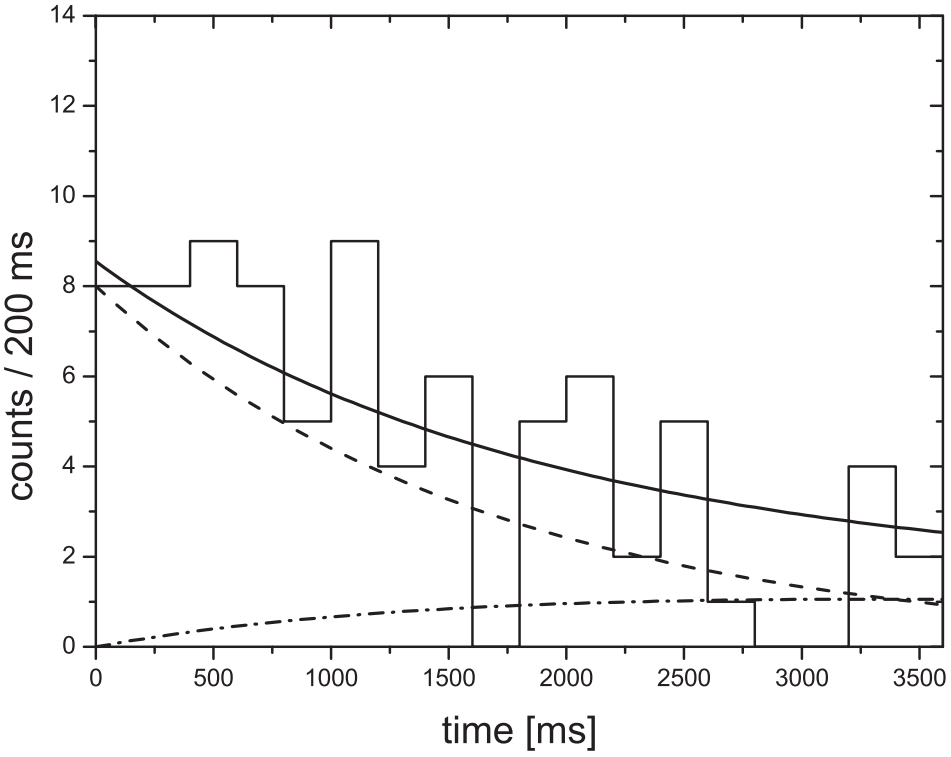

FIG. 2: Title: Time distribution of first decay events

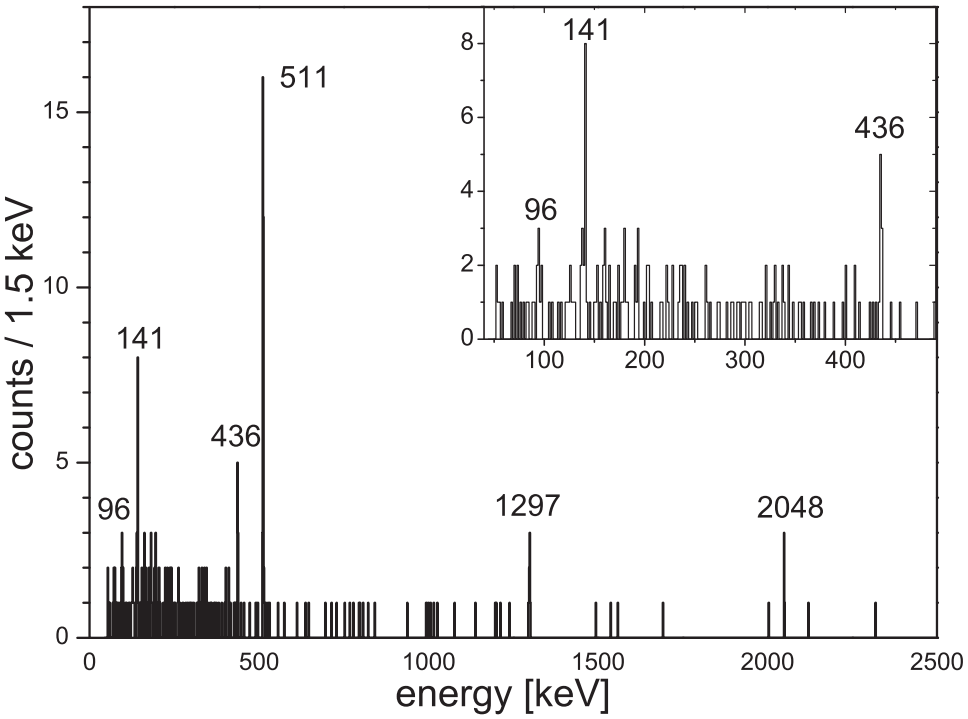

FIG. 3: Title: γ-radiation spectrum

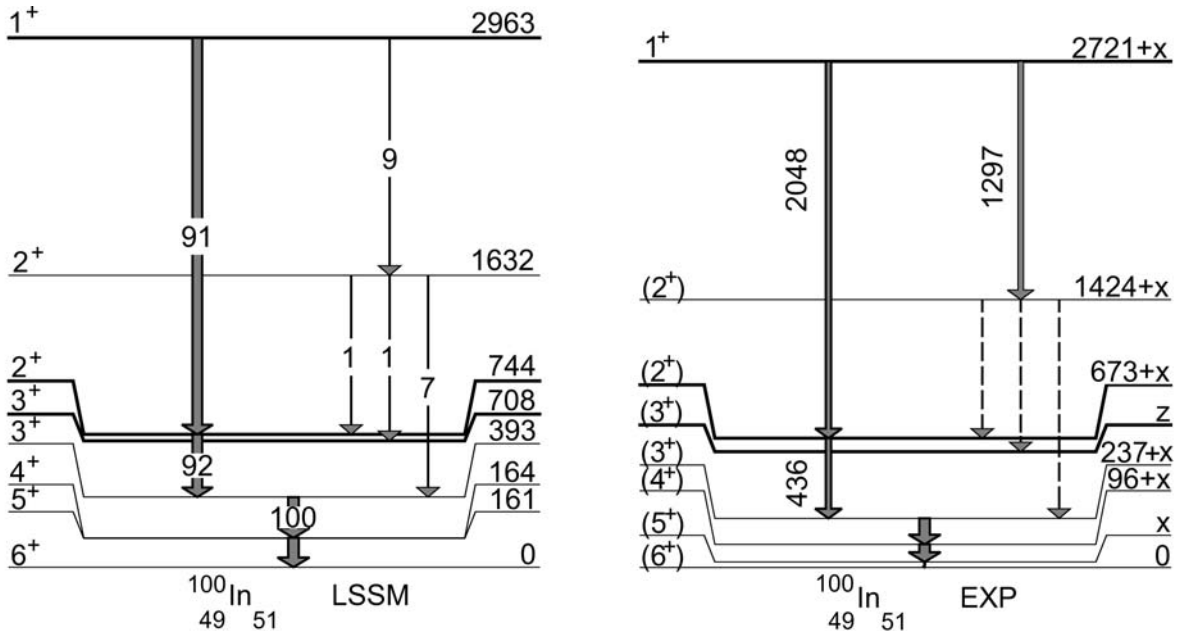

FIG. 4: Title: Tentative level scheme of ^{100}In

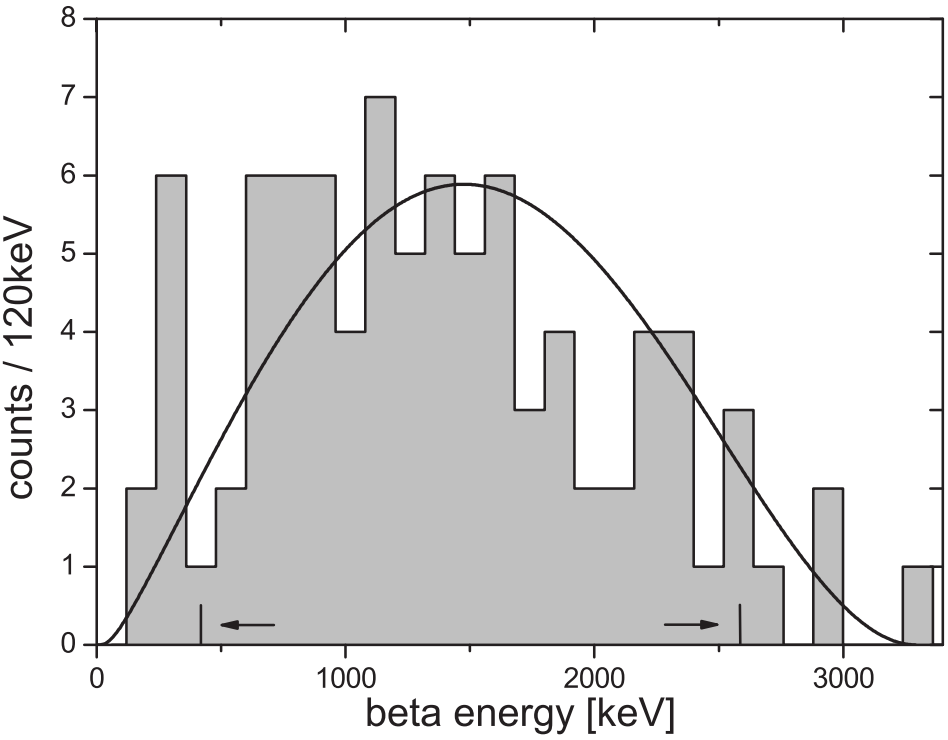

FIG. 5: Title: Distribution of positron energies

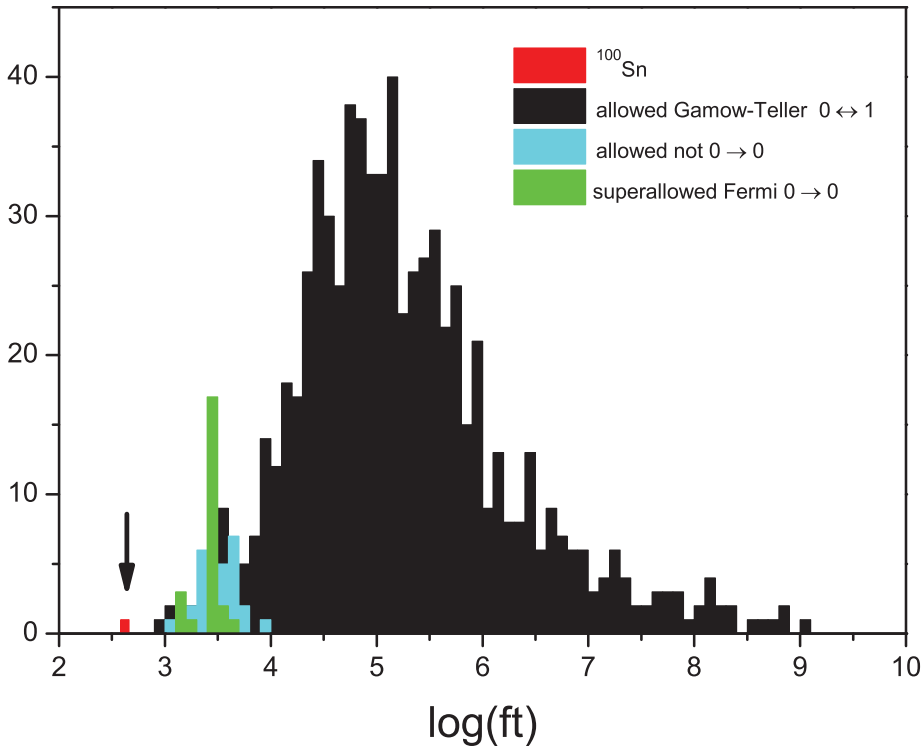

FIG. 6: Title: Log-ft values from allowed β-decays